Supplementary material

Immunoprecipitation (IP) and Western blot hybridization

Cells with 70 to 80% confluency were collected by centrifugation at 1800 rpm and washed with buffer 1 containing 50 mM Tris-HCl and 2 mM EDTA. Cells in buffer 1 were mixed with equal volume of high salt lysis buffer containing 600 mM NaCl, 50 mM Tris-HCl, 2 mM EDTA, 1% triton X100 and lysed for 30 min at 4^0C on a rotator. After lysis, the salt concentration was adjusted to 100mM for further IP by adding buffer 1. All IP buffers were supplemented with protease inhibitor cocktail tablets (Roche, 11873580001). The cell lysate was centrifuged at 12000 rpm for 20 minutes at 4^0C to remove cell debris and pre-cleared with Protein A magnetic beads for 1-2 hours before proceeding for IP. 10% of total cell lysate was retained as input. The diluted cell lysate (1500µl) was divided into equal halves, one was incubated with 3 µg of either rabbit polyclonal anti-dA2BP1 or rabbit polyclonal anti-Groucho or Goat anti-Su(H) (Santacruz) antibody and the other half was incubated with equal amount of Rabbit IgG (Bethyl) or Goat IgG (Santacruz) or Rat IgG (Santacruz), respectively as control. The mixture was rotated for 8-16 hours at 4^0C and further incubated with Protein A magnetic beads (Ademtech) for 3 hours. The beads were washed 4 times with 150 mM NaCl, 50 mM Tris-HCl, 2 mM EDTA, 0.1% triton-X and eluted in 50 µl wash buffer and 15 µl of 5X SDS loading buffer.

The protein sample was resolved by running 10% SDS-PAGE and blotted on PVDF membrane (Millipore). The blot was blocked with 5% fat-free milk in TBST buffer (20 mM Tris, pH 7.6; 150 mM NaCl; 1% Tween 20) and incubated with primary antibodies (diluted in blocking solution) either 3 hours at room temperature or overnight at 4^oC under rotating condition. After incubation, the primary antibodies were removed and the blot was washed 4 times with TBST, 10 minutes each. The blot was further incubated with secondary antibodies conjugated with HRP (diluted in blocking solution) for 1 hour at room temperature under rotating condition. After incubation, the secondary antibodies were removed and the blot was washed 4 times with TBST, 10 minutes each. Finally, the blot was exposed with HRP substrate (Millipore) and imaged by CCD camera LAS 4000. The images were processed with Image J or Fujifilm software.

Table S1. Statistics of comparison of sensory bristle numbers between wildtype and various experimental genotypes. Significant differences are represented as *** for *p*-value < 0.001, ** for *p*-value < 0.01, * for *p*-value < 0.05. Figure numbers of corresponding figures/graphs are indicated in the table. NS = Not Significant.

Genotypes	***p*-value**	**Significance**
Figure 1L		
Wildtype (n=30) ***vs*** *sca*G4> *dA2BP1*^{RNAi} (n=27)	5.64E-17	***
Wildtype (n=30) ***vs*** *sca*G4> UAS dA2BP1 (n=25)	2.41E-34	***
Figure 1M		
Wildtype (n=20) vs scaG4> dA2BP1RNAi (n=20)	4.19E-06	***
Wildtype (n=20) vs scaG4> UAS dA2BP1 (n=20)	0.01100	*
Figure 2		
*sca*G4>UAS GFP (n=7) ***vs*** *sca*G4> *dA2BP1*^{RNAi} (n=7)	0.0484	*
*sca*G4>UAS GFP (n=7) ***vs*** *sca*G4> UAS dA2BP1 (n=9)	2.07E-05	***
Figure 3G		
Wildtype (n=30) ***vs*** *N*^{55e11}/+ (n=25)	6.58E-11	***
Wildtype (n=30) ***vs*** *sca*G4> *dA2BP1*^{RNAi} (n=27)	5.64E-17	***
*sca*G4> *dA2BP1*^{RNAi} (n=27) ***vs*** *sca*G4> *dA2BP1*^{RNAi} / *N*^{55e11}(n=25)	1.19E-08	***
N^{55e11}/+ (n=25) ***vs*** *sca*G4> *dA2BP1*^{RNAi} / *N*^{55e11} (n=25)	1.15E-21	***
Wildtype (n=30) ***vs*** *N*^{Ax16}/+ (n=20)	4.13E-05	***
*sca*G4> *dA2BP1*^{RNAi} (n=27)***vs*** *sca*G4> *dA2BP1*^{RNAi} / *N*^{Ax16} (n=20)	4.24E-15	***
N^{Ax16}/+ (n=20) ***vs*** *sca*G4> *dA2BP1*^{RNAi} / *N*^{Ax16} (n=20)	7.44E-08	***
Figure 5E		
Wildtype (n=30) ***vs*** *sca*G4> *dA2BP1*^{RNAi} (n=27)	5.64E-17	***
Wildtype (n=30) ***vs*** *sca*G4/+; *H*^{1}/+ (n=23)	1.78E-10	***
*sca*G4/+; *H*^{1}/+ (n=23) ***vs*** *dA2BP1*^{RNAi} /+; *sca*G4/+; *H*^{1}/+ (n=22)	3.60E-07	***
Wildtype (n=30) ***vs*** *sca*G4/+; *H*^{2}/+ (n=28)	1.63E-13	***
*sca*G4/+; *H*^{2}/+ (n=28) ***vs*** *dA2BP1*^{RNAi} /+; *sca*G4/+; *H*^{2}/+ (n=28)	1.56E-12	***
Wildtype (n=30) ***vs*** *sca*G4/+; *H*^{3}/+ (n=24)	7.19E-13	***
*sca*G4/+; *H*^{3}/+ (n=24) ***vs*** *dA2BP1*^{RNAi} /+; *sca*G4/+; *H*^{3}/+ (n=16)	2.82E-06	***
Figure S3K		
Wildtype (n=30) ***vs*** *sca*G4> *dA2BP1*^{RNAi} (n=27)	5.64E-17	***
Wildtype (n=30) ***vs*** *c253*G4> *dA2BP1*^{RNAi} (n=48)	9.11E-20	***
Wildtype (n=30) ***vs*** *pnr*G4> *dA2BP1*^{RNAi} (n=31)	3.09E-18	***

Wildtype (n=30) ***vs*** *MS*^{248}G4> *dA2BP1*^{RNAi} (n=81)	7.95E-34	***
Wildtype (n=30) ***vs*** *ap*G4> *dA2BP1*^{RNAi} (n=71)	3.80E-14	***
Wildtype (n=30) ***vs*** *eyg*G4> *dA2BP1*^{RNAi} (n=66)	3.38E-18	***
Figure S6G		
Wildtype (n=30) vs scaG4> dA2BP1^{RNAi} *(n=27)*	5.64E-17	***
scaG4> dA2BP1^{RNAi} *(n=27) vs scaG4> dA2BP1*^{RNAi}*; sens*^{E2}*/+ (n=25)*	4.79E-11	***
scaG4> dA2BP1^{RNAi} *(n=27) vs scaG4> dA2BP1*^{RNAi}*; sens*^{58}*/+ (n=25)*	4.34E-13	***
Figure S8E		
*pros*G4> UAS GFP (n=20) ***vs*** *pros*G4> *dA2BP1*^{RNAi} (n=20)	0.15164	NS
*pros*G4> UAS GFP (n=20) ***vs*** *pros*G4/N^{DN} (n=20)	0.02707	*
*pros*G4> *dA2BP1*^{RNAi} (n=20) ***vs*** *dA2BP1*^{RNAi}; *pros*G4/N^{DN} (n=20)	0.43192	NS
*pros*G4/N^{DN} (n=20) ***vs*** *dA2BP1*^{RNAi}; *pros*G4/N^{DN} (n=20)	0.81928	NS

Supplemental Figures

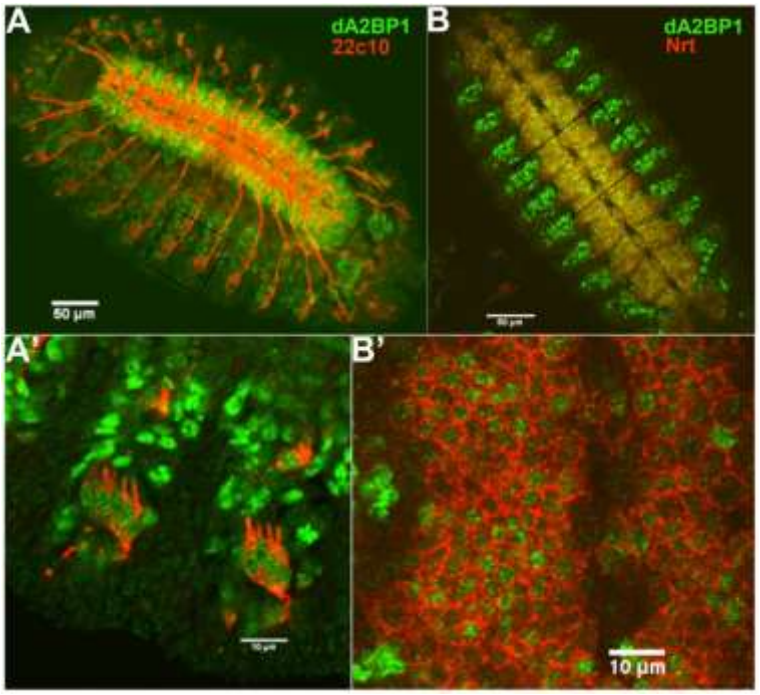

Figure S1. dA2BP1 is expressed in developing central and peripheral nervous systems of *Drosophila* embryos.

(A, B) Stage 14 embryos stained for dA2BP1 (green) and Futsch (22c10, red, A) or Neurotactin (Nrt, red, B). A' and B' show higher magnification images of A and B, respectively. Futsch marks peripheral nervous system, while Nrt marks the neuronal population of VNC.

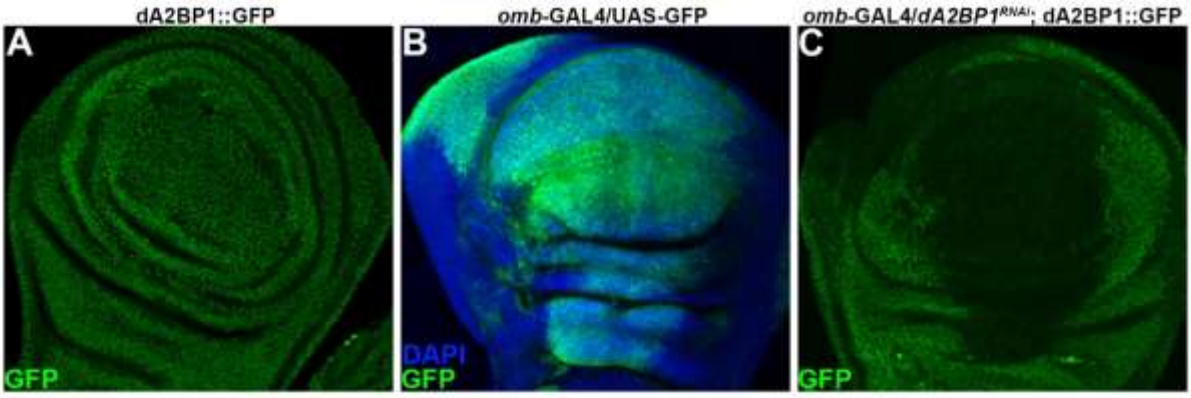

Figure S2. RNAi-mediated downregulation of dA2BP1 expression.

(A) dA2BP1::GFP wing disc of 3rd instar larvae showing wild-type expression pattern of dA2BP1. (B) *omb*-GAL4/UAS-GFP wing disc showing expression pattern of the omb-GAL4 driver in the 3rd instar larval stage. (C) *omb*-GAL4/UAS-*dA2BP1*^{RNAi}; dA2BP1::GFP wing disc showing down-regulation of *dA2BP1* in the entire region where RNAi is induced by the *omb*-GAL4 driver confirming the efficiency of the RNAi transgene.

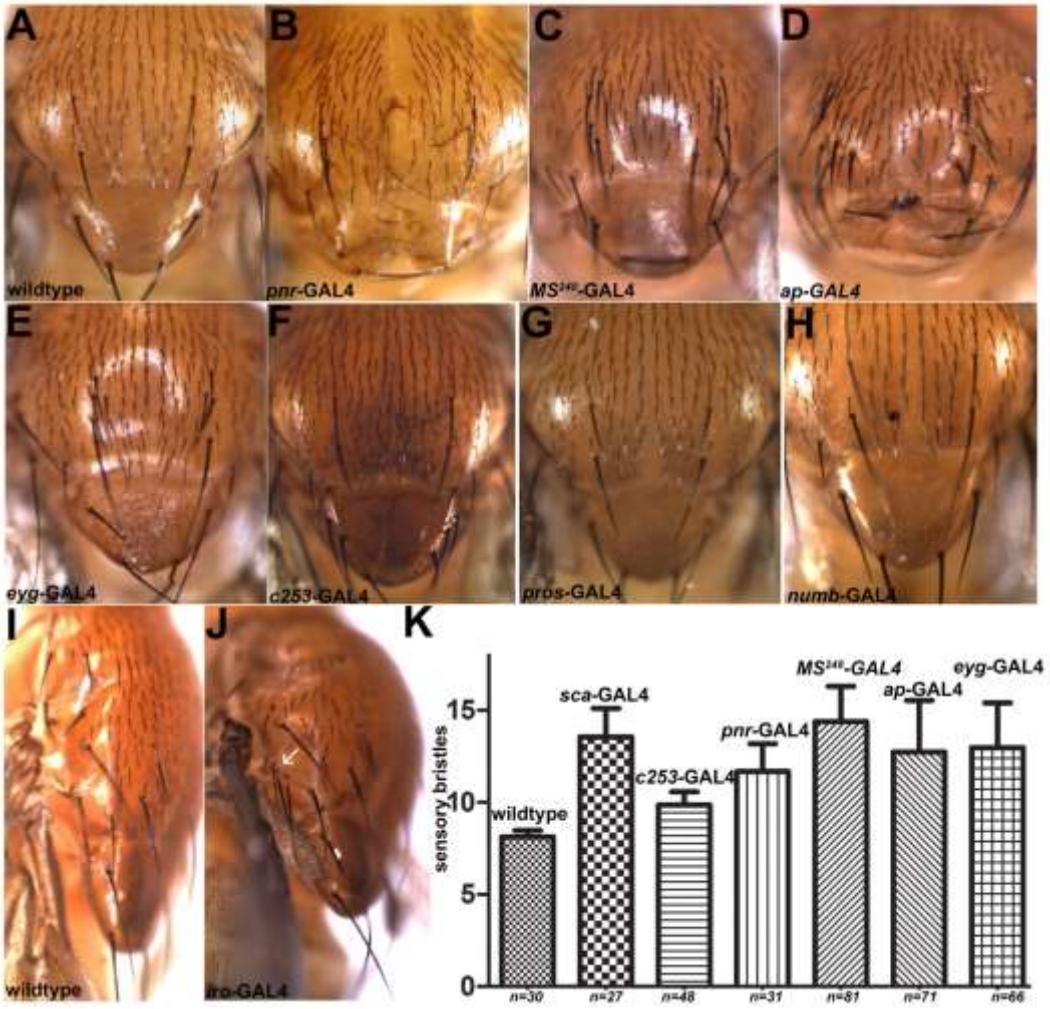

Figure S3. dA2BP1 loss of function causes increase in the number of sensory bristles on the *Drosophila* thorax.

(A-J) Adult thorax of *wildtype* (A, I), UAS-*dA2BP1*^{RNAi}*; pnr*-GAL4 (B), UAS-*dA2BP1*^{RNAi}*; MS*^{24B}-GAL4 (C), UAS-*dA2BP1*^{RNAi}*; ap*-GAL4 (D), UAS-*dA2BP1*^{RNAi}*; eyg*-GAL4 (E), UAS-*dA2BP1*^{RNAi}*; c253*-GAL4 (F), UAS-*dA2BP1*^{RNAi}*; pros*-GAL4 (G), UAS-*dA2BP1*^{RNAi}*; numb*-GAL4 (H) and UAS-*dA2BP1*^{RNAi}*; iro*-GAL4 flies (J). Arrow marks the increase in bristle at *iro*-GAL4 expressing region (J). Except with *numb*-GAL4 and *pros*-GAL4, *dA2BP1*^{RNAi}–mediated downregulation of dA2BP1 causes increase in bristle number. (L) Statistical analysis of changes in bristle number (DC + SC) in different genetic backgrounds. Error bars represent standard deviation. All genotypic combinations were significantly different than wild type at $p < 0.0001$.

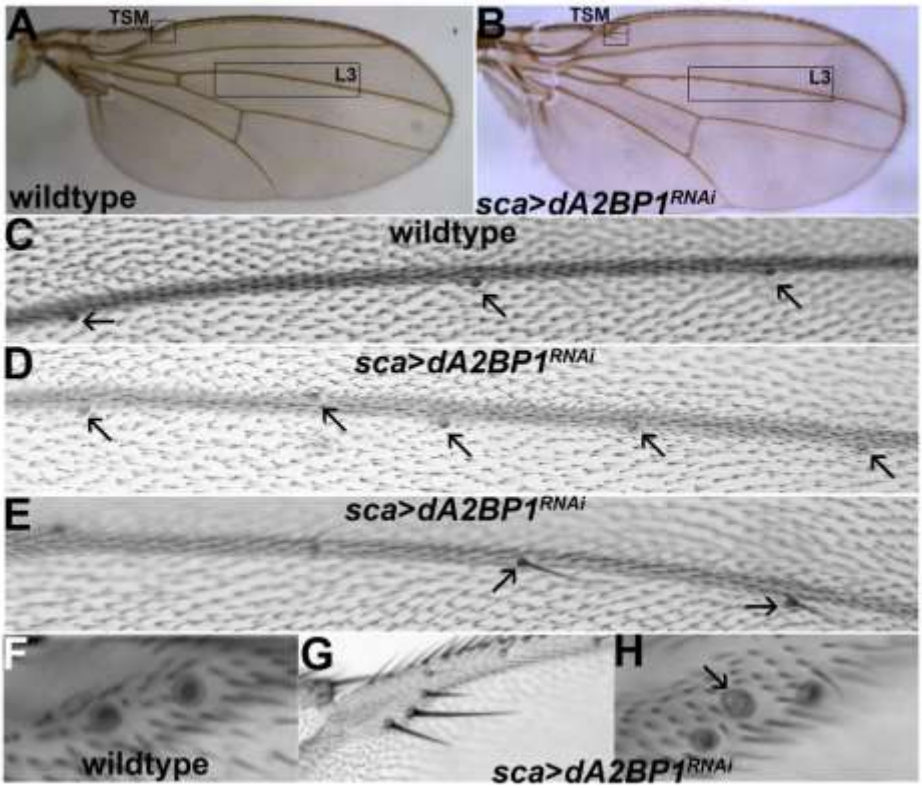

Figure S4. Downregulation of *dA2BP1* causes increase in campaniform sensilla number and its transformation to bristle type.

(A-B) Wildtype (A) and UAS-*dA2BP1*^{RNAi}*; sca*-GAL4 (B) wing blades marking the campaniform sensilla position; the L3 vein campaniform sensillum and the twin sensilla of the margin (TSM). Regions marked as L3 in A and B are shown at higher magnification in C and D, respectively. Please note 2 additional L3 vein campaniform sensilla (D). We also occasionally observed sensory bristles on L3 (E; image was taken from a different wing blade than shown in B). (F-G) A section of wild-type (F) and UAS-*dA2BP1*^{RNAi}*; sca*-GAL4 (G) wing blades showing twin sensilla of the margin at higher magnification. Note sensory bristles in the wing margin in the place of socketed sensory organs (G). In some wing blades, we also observed 3 sensilla in the place of normal two (H; image was taken from a different wing blade than shown in B).

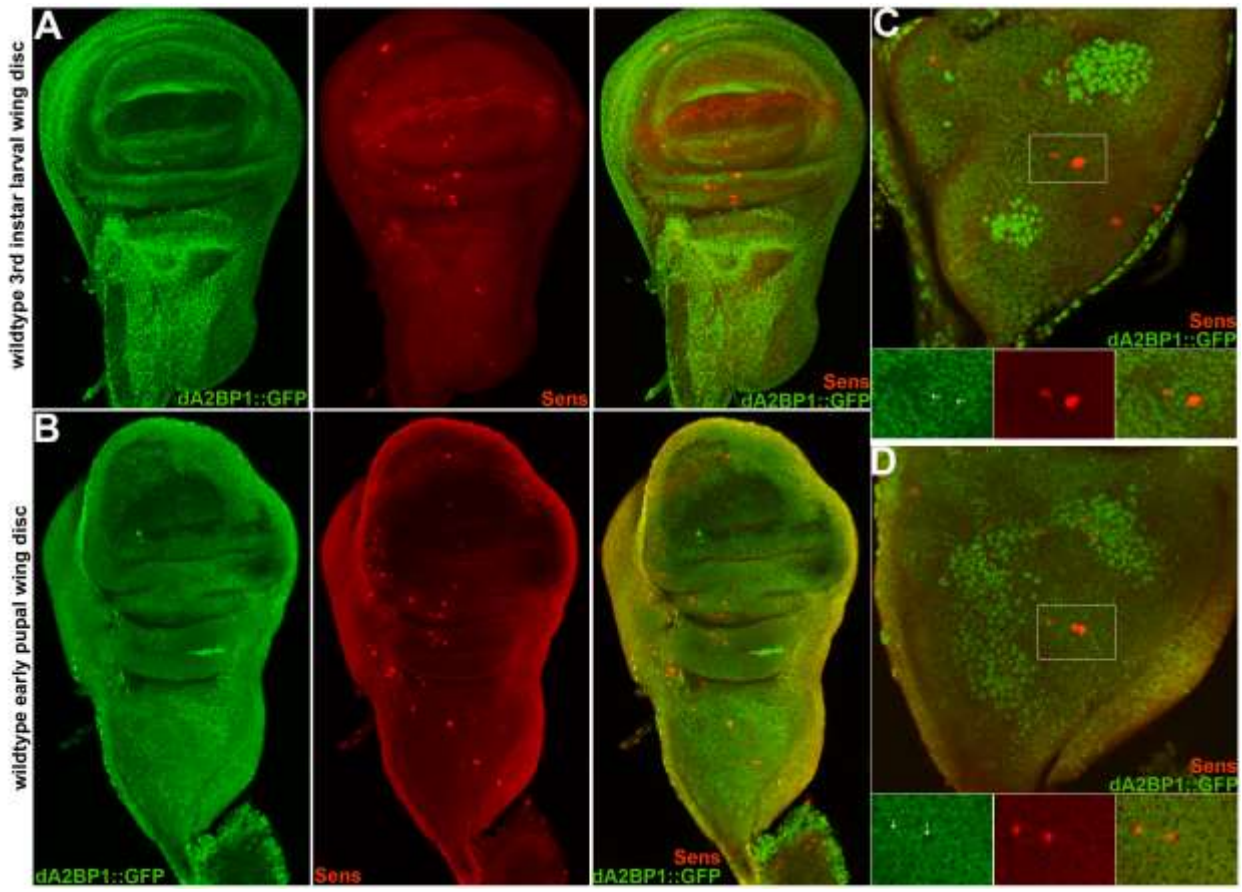

Figure S5. Reduced levels of dA2BP1 expression in the SOPs of pupal wing disc compared to larval stages.

(A) 3rd instar larval wing disc of dA2BP1::GFP showing the expression pattern of dA2BP1 and Sens. dA2BP1 expression is strong in most parts of the wing disc including SOPs, as marked by Sens. (B) Wing disc of dA2BP1::GFP at 4h after puparium formation showing the expression pattern of dA2BP1 and Sens. The discs have started everting as evidenced by wing margin expression pattern of Sens. Relative to larval stages, dA2BP1 expression is much lower in most parts of the wing disc including SOPs, as marked by Sens. Discs in A and B are at 20X magnification. (C-D) 3rd instar larval (C) and early pupal (D) discs at higher magnification (40X). Insets in both C and D show corresponding boxed region for better clarity of dA2BP1 expression in SOPs. In larval discs, all SOPs show dA2BP1 expression (arrows in C). At pupal stages, we did observe expression of dA2BP1, specifically in dividing SOPs (dotted arrow in D). Even at this stage, a SOP, which has not yet started dividing, still expresses dA2BP1 (arrow in D).

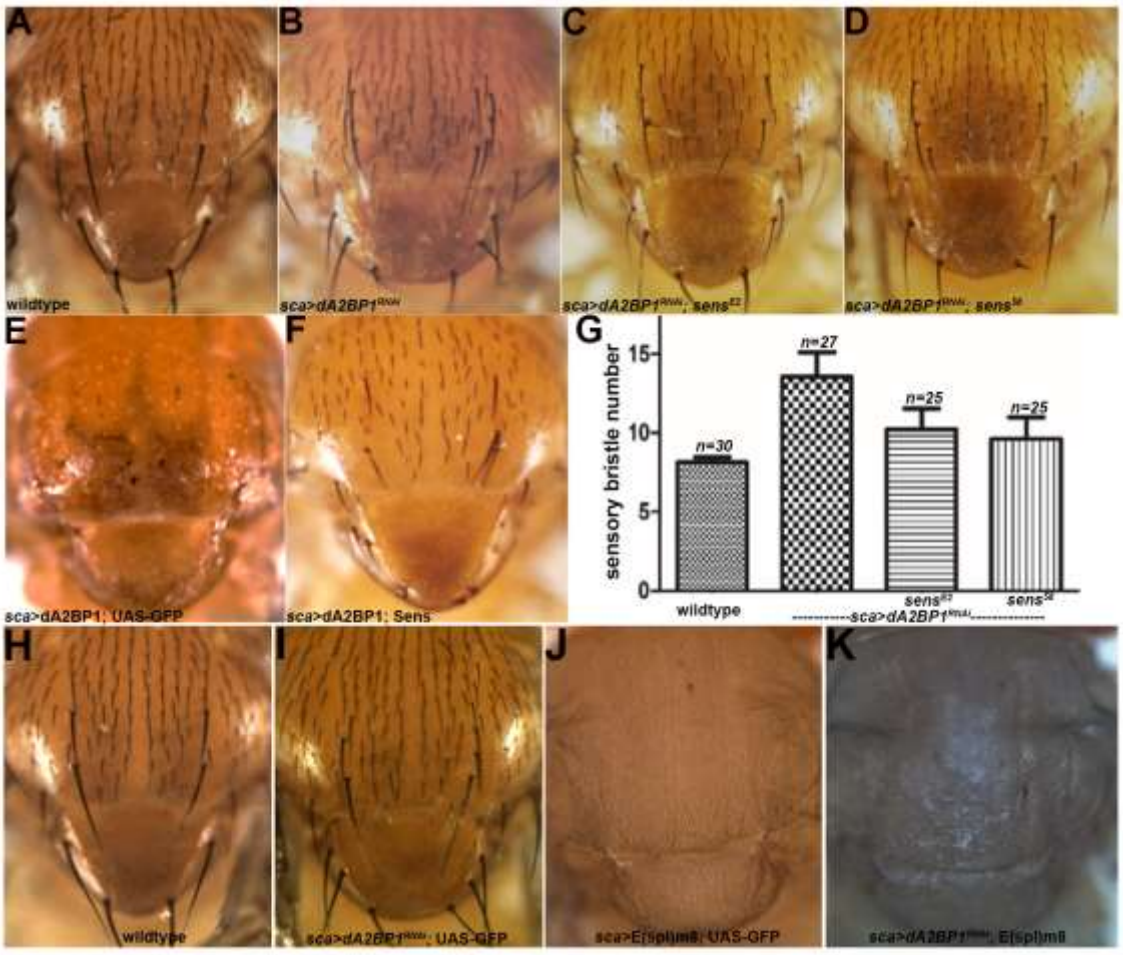

Figure S6. dA2BP1 is upstream of Senseless and E(spl)m8 in the Notch pathway

(A-D) Adult thorax of wildtype (A), UAS-*dA2BP1*^{RNAi}*; sca*-GAL4 (B), UAS-*dA2BP1*^{RNAi}*; sca*-GAL4; *sens*^{E2}/+ (C) and UAS-*dA2BP1*^{RNAi}*; sca*-GAL4; *sens*^{58}/+ (D) flies. *sens* heterozygous flies do not have any sensory bristle phenotype. *dA2BP1*^{RNAi}–induced supernumerary phenotype, however, is suppressed by heterozygous *sens* alleles. (E-F) Adult thorax of *sca*-GAL4/UAS-dA2BP1; UAS-GFP (E) and UAS-Sens; *sca*-GAL4/UAS-dA2BP1 (F). Over-expression of dA2BP1 results in loss of sensory bristle on the adult thorax (E). This phenotype is suppressed by the over-expression of Sens (F). (G) Statistical analysis of changes in bristle number (DC + SC) in different genetic backgrounds. Error bars represent standard deviation. Suppression of *dA2BP1*^{RNAi}–induced supernumerary phenotype is significant at $p<0.0001$. Numbers of adult thoraces examined are indicated against each genotype in the bar diagram.

(H-K) adult thorax of wildtype (H) UAS-*dA2BP1*^{RNAi}*; sca*-GAL4; UAS-GFP (I), *sca*-GAL4; UAS-E(spl)m8/UAS-GFP (J) and UAS-*dA2BP1*^{RNAi}*; sca*-GAL4; UAS-E(spl)m8 (K) flies.

Loss of dA2BP1 in super-numerary bristle phenotype, while over-expression of E(spl)m8 results in complete loss of both macrochaetae and microchaetae (J). The phenotype caused by the over-expression of E(spl)m8 is dominant to that of loss of function of dA2BP1 (K) suggesting that the E(spl)m8 is downstream of dA2BP1.

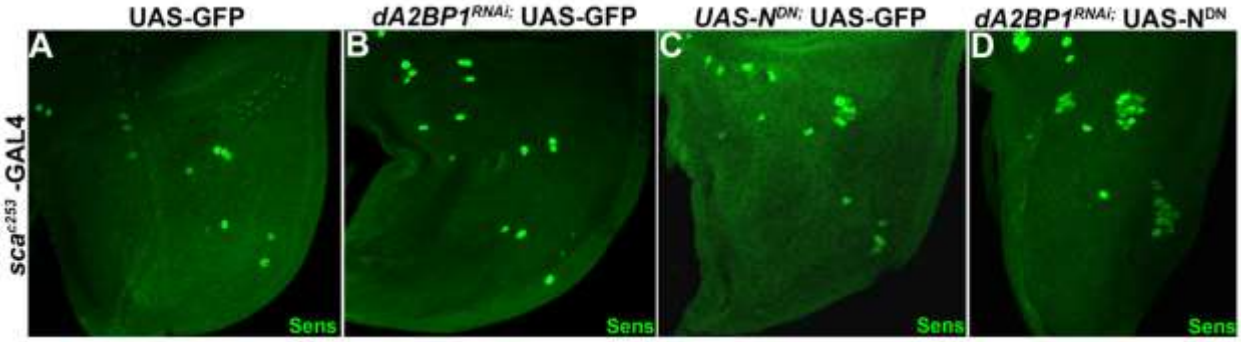

Figure S7. Increase in sensory bristles due to downregulation of both *dA2BP1* and N-is due to increase in the number of SOPs at the larval stages.

(A-D) *sca*^{c253}-GAL4; UAS-GFP (A), UAS-*dA2BP1*^{RNAi}; *sca*^{c253}-GAL4; UAS-GFP (B), UAS-N^{DN}/*sca*^{c253}-GAL4; UAS-GFP (C) and UAS-*dA2BP1*^{RNAi}; UAS-N^{DN}/*sca*^{c253}-GAL4 (D) wing imaginal discs stained for Sens expression. Note increase in the number of Sens-expressing cells. The large clusters of Sens-expressing cells in D corresponds to tufted bristles phenotypes seen in the adult thorax of the same genotype (Fig. 4G). This suggests increase in the number of SOPs in this genotypic combination rather than the just increase in external bristle cells of the sensory organs.

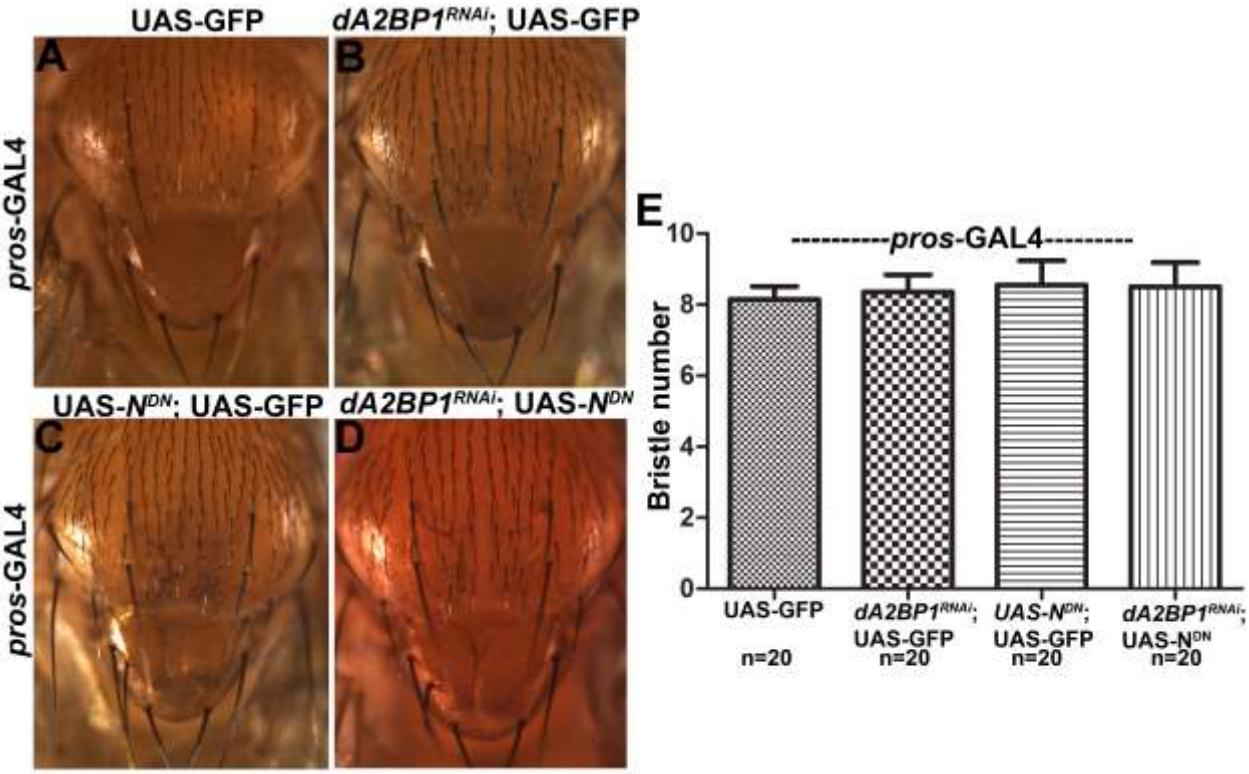

Figure S8. dA2BP1 has no role after the specification of SOPs.

(A-D) Images of adult thorax of *pros*-GAL4; UAS-GFP (A), UAS-*dA2BP1*^{RNAi}; *pros*-GAL4; UAS-GFP (B), UAS-N^{DN}/*pros*-GAL4; UAS-GFP (C) and UAS-*dA2BP1*^{RNAi}; UAS-N^{DN}/ *pros*-GAL4 (D). There is mild increase in the number or pattern of sensory bristles when N pathway is downregulated in late stages of SOP specification using *pros*-GAL4 driver. However, this phenotype is unaffected when *dA2BP1* is downregulated in this background.

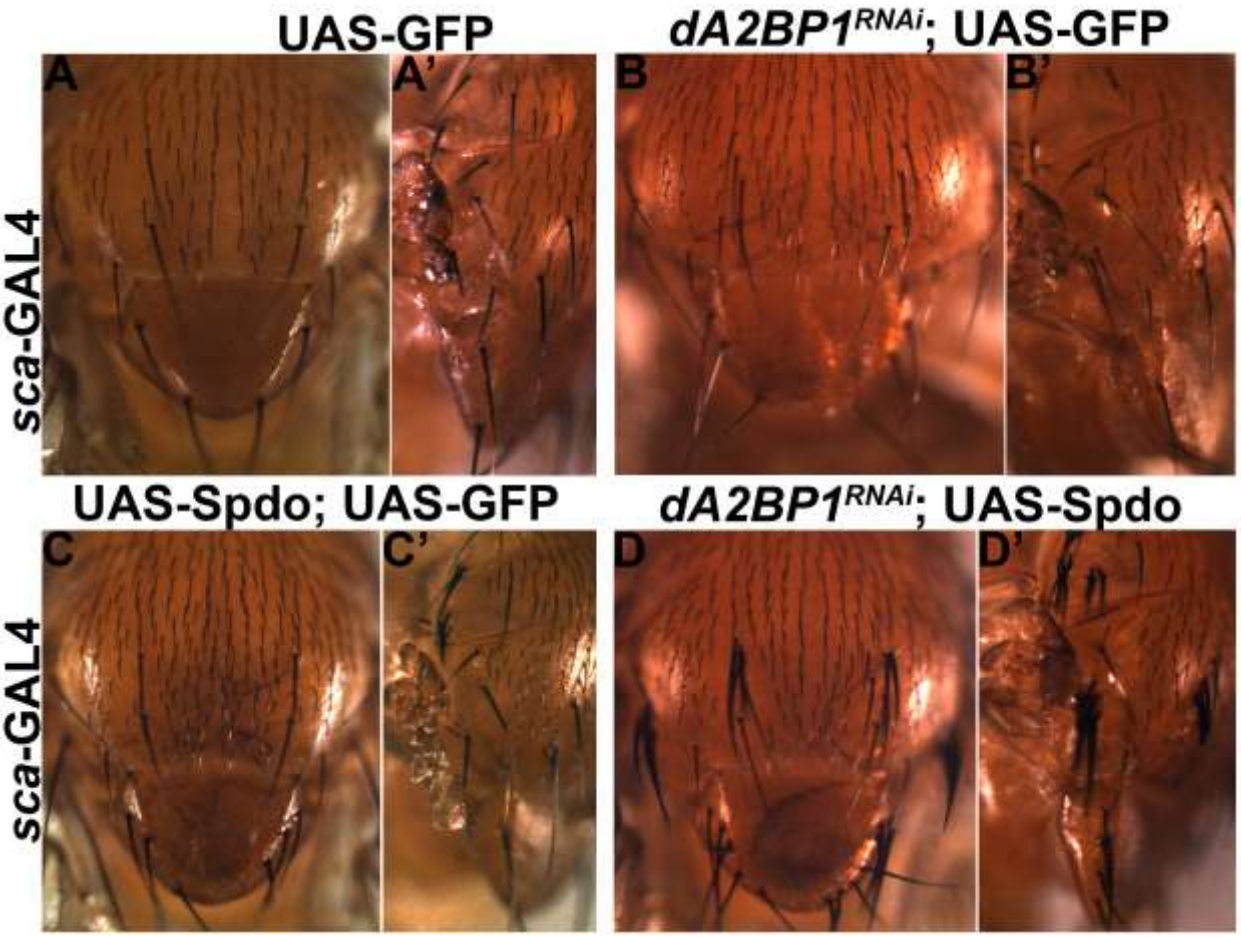

Figure S9. Loss of dA2BP1 enhances the phenotype caused by the over-expression of Sanpodo, a negative regulator of Notch pathway.

(A-D) Adult thorax of *sca*-GAL4; UAS-GFP (A), UAS-*dA2BP1*^{RNAi}; *sca*-GAL4; UAS-GFP (B), UAS-Spdo/*sca*-GAL4; UAS-GFP (C) and UAS-*dA2BP1*^{RNAi}; UAS-Spdo/*sca*-GAL4 (D). Note increase in the number of sensory bristles in both B and C, which is significantly further enhanced in D. The number of full sensory organs is increased rather than just bristles, as shown in D' at higher magnification.

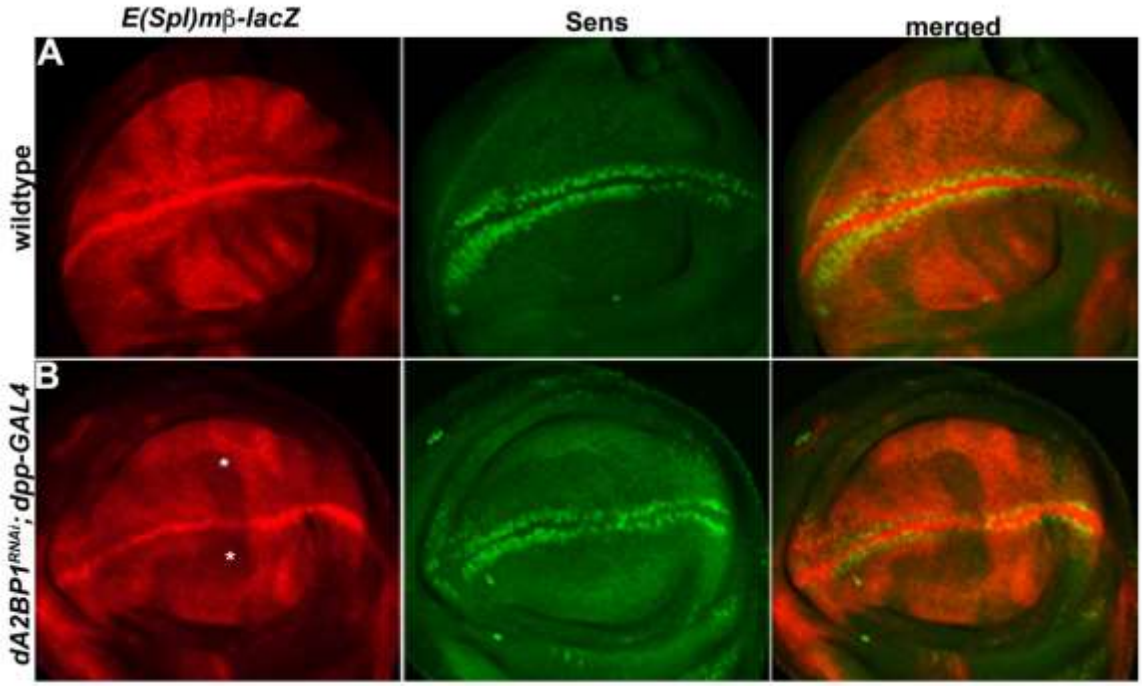

Figure S10. dA2BP1 regulates the expression of *E(spl)mβ* in wing epithelium

(A-B) *E(spl)mβ* –lacZ (A) and UAS-*dA2BP1*^{RNAi}*; E(spl)mβ* –lacZ*; dpp*-GAL4; (B) wing discs stained for lacZ and Sens expression. Downregulation of *dA2BP1* at the A/P boundary results in loss of *E(spl)mβ* expression in non-DV cells (white asterisks). Expression of *E(spl)mβ* in the D/V boundary, wherein dA2BP1 is not expressed (Bajpai et al., 2004) is unaffected.

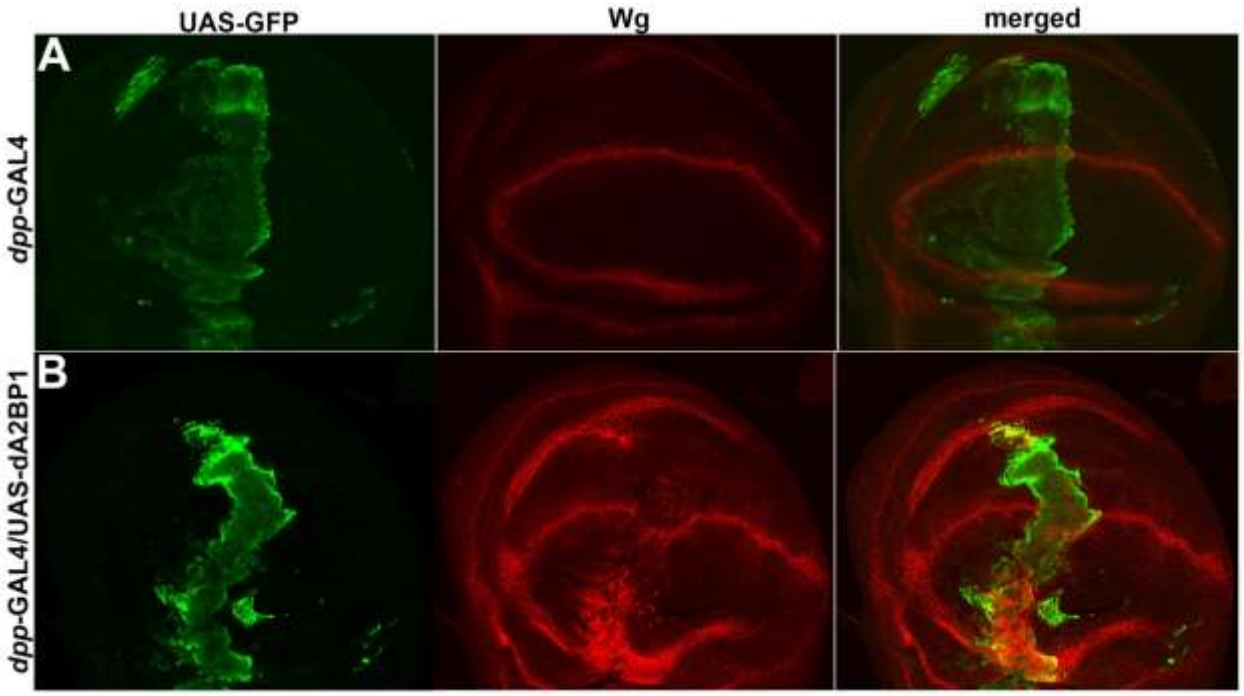

Figure S11. Ectopic expression of dA2BP1 activates Wg expression in wing epithelium

(A-B) *dpp*-GAL4/UAS-GFP (A) and UAS-dA2BP1; *dpp*-GAL4/UAS-GFP (B) wing discs stained for GFP and Wg expression. Upregulation of dA2BP1 at the A/P boundary results in the activation of Wg expression along the boundary, an indication of activation of N pathway.